

Allee dynamics: Growth, extinction and range expansion

Indrani Bose

Department of Physics, Bose Institute

93/1, Acharya Prafulla Chandra Road, Kolkata-700009, India

indrani@jcbose.ac.in

Mainak Pal

Department of Physics, Bose Institute

93/1, Acharya Prafulla Chandra Road, Kolkata-700009, India

mainakpl3@gmail.com

Chiranjit Karmakar

Department of Physics, Indian Institute of Technology Guwahati,

Guahati-781039, Assam, India

k.chiranjit@iitg.ernet.in

Abstract

In population biology, the Allee dynamics refer to negative growth rates below a critical population density. In this paper, we study a reaction-diffusion (RD) model of population growth and dispersion in one dimension, which incorporates the Allee effect in both the growth and mortality rates. In the absence of diffusion, the bifurcation diagram displays regions of both finite population density and zero population density, i.e., extinction. The early signatures of the transition to extinction at the bifurcation point are computed in the presence of additive noise. For the full RD model, the existence of travelling wave solutions of the population density is demonstrated. The parameter regimes in which the travelling wave advances (range expansion) and retreats are identified. In the weak Allee regime, the transition from the pushed to the pulled wave is shown as a function of the mortality rate constant. The results obtained are in agreement with the recent experimental observations on budding yeast populations .

Keywords : Allee effect; bistability; bifurcation point; early signatures of population extinction transition; travelling wave solution; pulled and pushed waves

PACS Nos.: 05.40.Ca , 05.45.-a , 87.15.Aa, 87.16.Uv

1. Introduction

Biological systems are characterised by dynamics with both local and non-local components. In the case of well-mixed systems, one needs to consider only local dynamics based on reaction/growth kinetics. The concentrations of biomolecules like messenger RNAs (mRNAs) and proteins increase through synthesis and decrease through degradation. The density of a cell population is subjected to changes brought about by birth and death processes. In the latter case, depending upon specific conditions, the cell population acquires a finite density in the course of time or undergoes extinction. In the case of a spatially extended system, reaction-diffusion (RD) processes govern the dynamics of the system. The RD models have been extensively studied in the context of spatiotemporal pattern formation in a variety of systems [1, 2]. One possible consequence of RD processes is the generation of travelling waves which are characteristic of a large number of chemical and biological phenomena [3, 4]. The shape of a travelling wave is invariant as a function of time and the speed of propagation is a constant. Biological systems exhibit travelling waves of measurable quantities like biochemical concentration, mechanical deformation, electrical signal, population density etc. One advantage of travelling fronts in biological systems is that for communication over macroscopic distances, the propagation time is much shorter than the time required in the case of purely diffusional processes. In this paper, we study cell population dynamics in a one dimensional (1d) spatially extended system described by the RD equation with the general form

$$\frac{\partial u(x, t)}{\partial t} = D \frac{\partial^2 u}{\partial x^2} + F(u) \quad (1)$$

where $u(x, t)$ denotes the population density at the spatial location x and time t , D is the diffusion coefficient and the term $F(u)$ represents the local growth rate incorporating the Allee effect [4, 5, 6] implying reduced per capita growth rates at low population densities. In the case of the strong Allee effect, the growth rates becomes negative below a critical population density resulting in

population extinction. The specific form of $F(u)$, proposed in an earlier study [7], is given in Eq.(10). The focus of the study was to investigate the outcome of the combined processes of the Allee effect and the collective movement of the population through diffusion between the patches of a fragmented habitat. In our study, the continuous space RD model is investigated for the first time and we demonstrate the utility of the model in addressing issues like population growth, extinction and range expansion *vis-à-vis* some recent experimental observations on laboratory populations of budding yeast [8, 9, 10, 11].

2. Models of Growth and Extinction

In the absence of diffusion, only the the local dynamics of the population are relevant and the major issue of interest is the survival or extinction of the population in the steady state. In the case of logistic growth [3],

$$F(u) = \rho u \left(1 - \frac{u}{K}\right) \quad (2)$$

where ρ denotes the exponential growth rate and K the carrying capacity (the population growth stops when $u = K$). The growth rate $F(u)$ satisfies the properties

$$F(0) = F(K) = 0 \quad (3)$$

with the steady state $u = 0$ being unstable and the steady state $u = K$ being stable, a case of monostability.

Also,

$$F(u) > 0 \text{ for } 0 < u < K, \quad F(u) < 0 \text{ for } u > K \quad (4)$$

$$F'(0) = \rho > 0, F'(u) < \rho \text{ for } u > 0 \quad (5)$$

where the prime represents the derivative with respect to u . The per capita growth rate, $f(u) = \frac{F(u)}{u}$, is a monotonically decreasing function of the population density, i.e., the per capita growth rate has a negative dependence on the population density. One common departure from the logistic growth, observed in natural and laboratory populations, is designated as the Allee effect [4, 5, 6] with positive dependence of the per capita growth rate on the population density till the maximal population density is achieved. In the case of the strong Allee effect, the local growth rate $F(u)$ is negative when the population density u is less than a critical density θ known as the Allee threshold. The negative growth rate results in population extinction in the long time limit. The most well-studied functional form of $F(u)$, which illustrates the Allee effect, is

$$F(u) = \rho u (u - \theta) \left(1 - \frac{u}{K}\right) \quad (6)$$

One now has

$$F(0) = F(\theta) = F(K) = 0 \quad (7)$$

with the steady states $u = 0$ and $u = K$ being stable, a case of bistability, and the state $u = \theta$ being unstable. The other conditions on $F(u)$ are

$$F(u) < 0 \text{ for } 0 < u < \theta \text{ and } u > K \quad (8)$$

$$F(u) > 0 \text{ for } \theta < u < K \quad (9)$$

The per capita growth rate $f(u)$ is negative below the Allee threshold and reaches a maximum value at an intermediate density. In the case of the weak Allee effect, the per capita growth rate is always positive signifying the absence of an Allee threshold. The maximal value again occurs at the intermediate density. A possible origin of the Allee effect lies in the reduced cooperativity amongst the individuals of the population at low population densities [5, 6, 12]. Examples include mate shortages in sexually reproducing species, less efficient feeding and reduced effectiveness of vigilance and antipredator defences [5, 6]. Allee effects have been demonstrated in all major taxonomic groups of animals, in plants[6] as well as microbial populations [8, 13].

There are several ways of modelling the Allee effects [4, 14] with most of the models explicitly including the Allee threshold as a parameter such that the per capita growth rate is negative (positive) below (above) the threshold. A less phenomenological model has been proposed by Berec *et al.* [7] which incorporates the Allee effect in both the birth (reproduction) and death (mortality) processes. The function $F(u)$ in this case is given by

$$F(u) = (\rho + \alpha u) u \left(1 - \frac{u}{K}\right) - \frac{\beta u}{1 + \frac{u}{\sigma}} \quad (10)$$

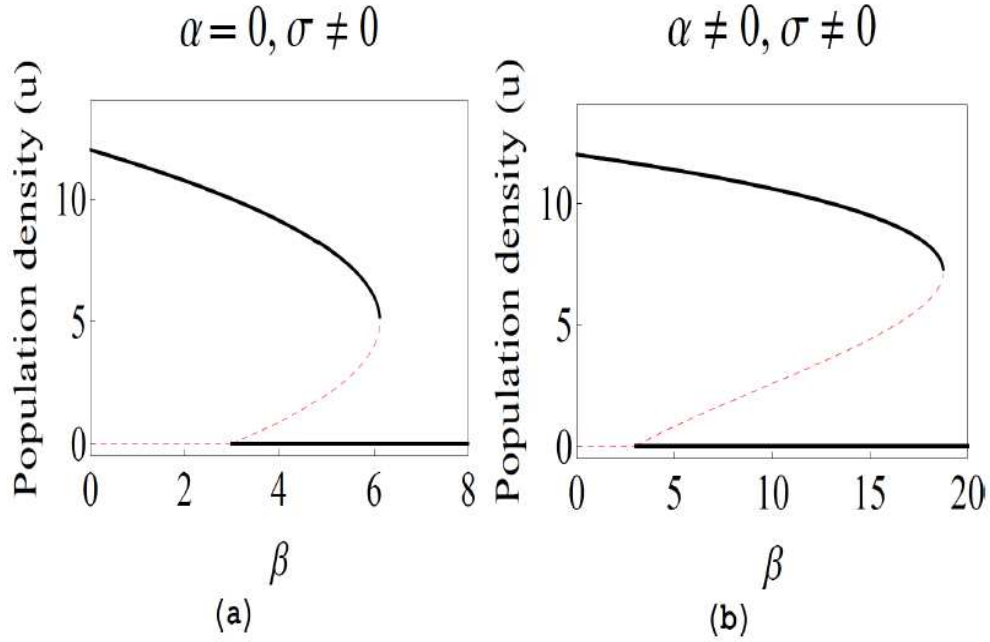


Fig. 1 Steady state population density u versus the mortality rate constant β for the cases (a) $\alpha = 0$ and (b) $\alpha = 1.0$ The other parameter values are $\rho = 3.0$, $K = 12.0$, $\sigma = 2.0$.

where ρ is the basic birth rate, α is the Allee effect coefficient with higher values of α signifying steeper increases in the reproduction rate, β denotes the mortality rate constant when the Allee effect is present, i.e., the per capita mortality rate increases (decreases) when the population density u approaches zero (increases) and the parameter σ is the population density for which the mortality rate is halved. If $\alpha = 0$ ($\sigma = 0$), there is no Allee effect on reproduction (mortality). If both the parameters α and σ are zero, the model reduces to the usual logistic growth model. In this paper, we study the RD model described in Eq. (1) with the functional form of $F(u)$ as given in Eq. (10). Though the model is of a general nature, our focus in this paper is on microbial populations, motivated by some recent experiments on laboratory populations of budding yeast [8, 9, 10, 11].

3. Allee Dynamics

We first report on the steady state properties of the model in the absence of diffusion. Figures 1(a) and 1(b) exhibit the steady state population density u versus the mortality rate constant β for the cases $\alpha = 0$ and $\alpha = 1$ respectively. In the region of bistability, the two stable state branches, represented by solid lines, are separated by a branch of unstable steady states, denoted by a dashed line. The upper stable steady state represents a population with finite density whereas the lower stable steady state ($u = 0$) corresponds to population extinction. The transitions between the bistable and monostable regions occur via the saddle-node (fold) bifurcation at two bifurcation points. In the region of bistability, if the initial population density is above the dotted line, the population acquires a finite density in the steady state. The population undergoes extinction if the initial population density falls below the dotted line. When $\alpha = 0$ the steady states are given by

$$u_1 = 0, u_2, u_3 = \frac{1}{2} \left[(K - \sigma) \pm \sqrt{(K + \sigma)^2 - \frac{4K\sigma}{\rho} \beta} \right] \quad (11)$$

with u_1, u_2 being stable and u_3 unstable. The region of bistability is obtained in the parameter regime

$$\rho < \beta < \frac{\rho (K + \sigma)^2}{4 \sigma K} \quad (12)$$

The boundary points of the regime represent the two bifurcation points. When $\alpha \neq 0$ (Fig. 1(b)), one obtains the steady states through numerical computation. As depicted in Figs. 1(a) and 1(b), a tipping point transition occurs at the upper bifurcation point from a finite population density to population collapse.

3.1 Early signatures of regime shifts

Recently, a large number of studies have been carried out on the early signatures of tipping point transitions involving sudden regime shifts in systems as diverse as ecosystems, financial markets, population biology, complex diseases, gene expression dynamics and cell differentiation [15, 16, 17, 18]. The early signatures include the critical slowing down and its associated effects, namely, rising variance and the lag-1 autocorrelation function as the bifurcation point is approached. Other signatures have also been proposed, e.g., an increase in the skewness of the steady state probability distribution as the system gets closer to the transition point [15, 16]. For our model system ($\alpha \neq 0, \beta \neq 0$), we compute the variance and the autocorrelation time (measures the time scale of correlation between the fluctuations at different time points), through simulation of the stochastic difference equation

$$u(t + \Delta t) = u(t) + F(u)\Delta t + \Gamma \xi \sqrt{\Delta t} \quad (13)$$

where $F(u)$, with the form given in Eq. (10), is computed at time t and the last term on the right hand side represents the effect of stochasticity (noise). Γ is the strength of the additive noise and ξ represents a Gaussian random variable with zero mean and unit variance. Let $\delta u(t) = u(t) - u_2$ represent the deviation of the population density u at time t from the stable steady state population density u_2 . The simulation data are recorded after 1000 time steps (stationarity conditions reached) for an ensemble of five hundred replicate populations. Fig. 2A shows the plots of $\delta u(t + \Delta t)$ versus $\delta u(t)$ for two distinct values of the bifurcation parameter β . The first figure depicts the results far from the bifurcation point, $\beta = 18.79$. The parameter values are $\Delta t = 0.01$ and $\Gamma = 0.5$ with the other parameter values the same as in Fig. 1(b). Figures. 2B and 2C display the autocorrelation time τ and the steady state sample variance σ^2 as a function of the parameter β . The autocorrelation time τ is computed as $\rho = e^{-\frac{1}{\tau}}$ where ρ is the lag-1 autocorrelation estimated by the sample Pearson's correlation coefficient [8].

$$\rho = \frac{1}{n-1} \frac{\sum_{i=1}^n (u_i(t) - \langle u_t \rangle)(u_i(t + \Delta t) - \langle u_{t+\Delta t} \rangle)}{S_{u_t} S_{u_{t+\Delta t}}} \quad (14)$$

where i denotes the sample index, n is the total number of samples, $\langle u_t \rangle$ is the sample mean and S_{u_t} the sample standard deviation at time t . In the computation, $n = 500$ and the time interval Δt is treated as the unit time interval.

Fig. 2 provides numerical evidence that both the variance and the autocorrelation time increase as the bifurcation point is approached. The return time equals the autocorrelation time [8] and its increase in the vicinity of the bifurcation point implies the critical slowing down. The results obtained in our model study are in accordance with the experimental observations of Dai *et al.* [8] on laboratory populations of budding yeast *S cerevisiae*. In the experiment, the Allee effect was realized through the cooperative growth of budding yeast in sucrose. Yeast cells are known to secrete an enzyme to hydrolyze extracellular sucrose outside the cell thus creating a common pool of the hydrolysis products, namely, glucose and fructose, which are then transported into individual cells for utilization in growth processes. The cooperative breakdown of sucrose results in the per capita growth rate becoming maximal at the intermediate cell densities when the competition for resources is not severe, a feature of the Allee effect. Replicate yeast cultures with a wide range of initial cell densities were subjected to daily dilutions into fresh sucrose media. The dilution is equivalent to introducing mortality in the population with higher dilution factors implying larger mortality rates. An experimental bifurcation diagram depicting the population density versus the dilution factor, which serves as the bifurcation parameter, was mapped out. The bifurcation was of the saddle-node type and a tipping point transition from a population of finite density to population extinction was identified. A simple two-phase growth model provided a good fit to the experimental data. In the model, the population growth was slow exponential at low densities and faster logistic at larger densities, based on experimental evidence. The theoretically predicted early warning signals of the tipping point transition were also tested experimentally. The experimentally obtained bifurcation diagram and the early warning signatures (Fig. 1(E) and Fig. 3 of Ref. 8) are qualitatively similar to the theoretical plots (Figs. 1 and 2) computed in our model study. The model serves as a microscopic model to describe population growth and extinction in the budding yeast population and explicitly includes the parameters describing the growth, the mortality and the Allee effect.

4. Reaction- Diffusion Model with Allee Dynamics

We next consider the full RD model shown in Eq.(1). Depending on the form of $F(u)$, two prototype cases are possible, monostability and bistability. The RD equation with $F(u)$ given in Eq. (2) (logistic growth), was first considered by Fisher [19] to describe the spread

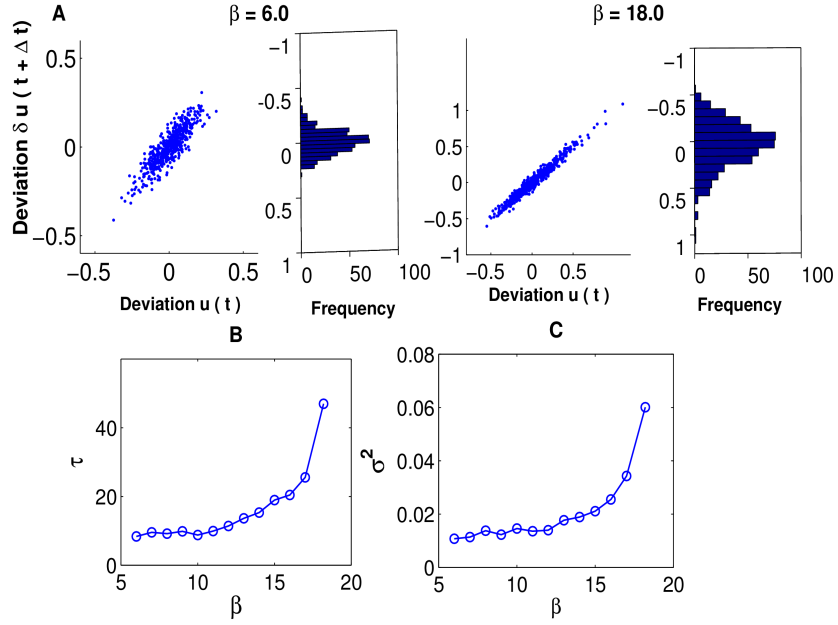


Fig. 2 A. Temporal correlations and frequency distributions of deviations from the stable steady state at $\beta = 6.0$ and $\beta = 18.0$. B and C. Plots of autocorrelation time τ and steady-state variance σ^2 as a function of β .

of a favourable gene in a population. The equation describes monostability and is referred to as the Fisher-Kolmogorov, Petrovskii and Piskunov (FKPP) equation. When $F(u)$ is of the form given in Eq. (6) and the conditions in Eqs. (8) and (9) hold true, i.e., the strong Allee effect is considered, the situation is that of bistability. It has been rigorously shown [4, 20] that for suitable initial conditions $u(x, 0)$, the disturbance evolves into a monotonic travelling front $u = q(x - ct)$, with constant speed c , joining the stable steady state with finite population density to the steady state $u = 0$ (unstable in the case of monostability and stable in the case of bistability). Populations occupy new territory through a combination of local growth and diffusion. If the population front moves from a region of finite u to one with $u = 0$, the phenomenon is characterised as a range expansion or invasion. If the travelling front moves in the opposite direction, the population retreats rather than advances.

In the case of the FKPP equation describing generalized logistic growth, a travelling wave solution with speed c satisfies the relation $c \geq c_{min}$ with

$$c_{min} = 2\sqrt{\rho D} \quad (15)$$

It has been shown that in the case of a compact initial condition, the initial population distribution always develops into a travelling population front with the minimum speed $c = c_{min}$. The scaling $c \propto \sqrt{\rho D}$ is known as the Luther formula [21] and holds true over many orders of magnitude in many chemical and biological systems [22]. A recent example pertains to the propagation of gene expression fronts in a one-dimensional coupled system of artificial cells [22]. We next consider the case of reaction-diffusion incorporating the Allee effect. When the strong Allee effect conditions prevail, i.e., $0 < \theta < K$ in Eq. (6), the travelling wave front has a unique speed given by [3, 14, 20]

$$v = \sqrt{\frac{D\rho}{2K}}(K - 2\theta) \quad (16)$$

In contrast to the case of logistic growth in which the travelling front has a finite value for the minimum speed, the speed v becomes zero at the so-called Maxwell point $\theta = \frac{K}{2}$ with reversal in the direction of motion of the travelling wave as the Maxwell point is

crossed. Also, the front has a unique speed instead of a spectrum of possible values above or equal to a minimum speed. If θ and K are treated as general parameters without any specific physical interpretation, then the parameter regions $0 < \theta < K$ and $-K < \theta < 0$ are associated with the strong and weak Allee effects respectively. For $\theta \leq -K$, the Allee effect is absent and the growth rate is of the generalized logistic type. Note that the parameter θ can no longer be treated as critical density when it assumes negative values.

In the case of the FKPP equation, the minimal speed of the travelling front can be written as $c_{min} = 2\sqrt{F'(0)D}$. The travelling wave is designated as the pulled wave with the wave speed depending solely on the growth rate at low population density and the diffusion coefficient [11]. The expansion is dominated by the dynamics at low population density prevailing at the very edge of the expanding wavefront which pulls the wave forward. The solution with the minimal speed defines the critical front while the solutions for which the wave speed c is $> c_{min}$ define the super-critical front. In the case of a pushed wave, the minimal speed satisfies the relation

$$c_{min} > 2\sqrt{F'(0)D} \quad (17)$$

The speed of the travelling front is now determined by the whole front rather than by only the leading edge. In the monostable case (weak Allee effect), the travelling front can be classified as either pulled or pushed wave whereas in the case of bistability (strong Allee effect), the travelling wave is always a pushed wave with a unique speed greater than $2\sqrt{F'(0)D}$. The theoretical prediction of a pulled to pushed wave transition [14] has recently been verified by Gandhi *et al.* [11] in a laboratory population of budding yeast as the cooperativity in growth was increased. The transition occurred at some intermediate magnitude of the Allee effect in the regime corresponding to the weak Allee effect.

The RD model studied in this letter with $F(u)$ as given in Eq. (10), has a more general form than the model most often studied in the context of the Allee effect ($F(u)$ as given in Eq. (6)). The existence of a travelling wave solution in this model is supported by the theorem proposed by Fife and McLeod [23]. The theorem states that the RD Eq. (1), with $F(u_1) = F(u_2) = F(u_3) = 0$ and $F'(u_1) < 0$, $F'(u_2) < 0$, $F'(u_3) > 0$, has a travelling wave solution $u(x, t) = U(x - vt)$ for exactly one value of the wave speed v . The solutions u_1 and u_2 describe stable steady states and the solution u_3 an unstable steady state. Also, $U(-\infty) = u_2$ and $U(+\infty) = u_1$, i.e., the travelling wave connects u_1 and u_2 . We assume that the parameter $\alpha = 0$ in Eq. (10), i.e., the Allee effect is present only in the mortality rate. In this case, the analytic solutions for the steady states are known (Eq. (11)) and one can look for travelling wave solutions for the RD equation. In the following, we report on the results obtained from numerical computations.

4.1 Range expansion, pushed and pulled waves

The 1d RD system has boundaries located at $-L$ and $+L$ respectively. We solve the RD equation on Mathematica with the compact initial conditions

$$u(x, t) = u_2 \quad \text{if } x \leq 0 \quad (18)$$

$$u(x, t) = u_1 \quad \text{if } x > 0 \quad (19)$$

The value of L is chosen to be 50, the diffusion coefficient $D = 1$ and the other parameter values are the same as in Fig. 1(a). Fig. 3 shows the computed travelling wave solutions at the time points $t = 20, 40, 60$ and 80 and $\beta = 5$. The front moves from the left to the right with the population of finite density, u_2 , advancing into the empty region, $u_1 = 0$. Fig. 4 shows the speed v of the travelling wave versus the mortality rate parameter β (solid circles). The speed was computed by plotting the midpoint x_m of the density profile versus time t and determining the slope of the straight-line fit [10]. The larger solid black circles represent the speed given by the formula, $v = 2\sqrt{F'(0)D} = 2\sqrt{(\rho - \beta)D}$, which corresponds to the speed of a pulled wave. The computed speed of the travelling wave and that of the pulled wave are nearly equal up to a transition point located within the big circle. The RD equation reduces to the FKPP equation when the parameter $\beta = 0$. In the case of compact initial conditions, as given in Eqs. (18) and (19), the exact expression for the travelling wave speed is that of the pulled wave. The small difference with the computed value can be ascribed to the finite size of the system and the small but finite errors associated with the numerical computation of speed. For $\beta < \rho = 3$, the system is monostable corresponding to the weak Allee effect regime. The strong Allee effect regime is bistable with the parameter range as specified in Eq. (12). At the transition point, $\beta \approx 1.823$, the travelling wave changes its nature from the pulled to the pushed wave. The speed of the travelling wave becomes zero at the Maxwell point $\beta_{MP} \approx 5.6259$. The travelling wave then reverses its direction, i.e., the wave retreats from the empty region rather than advance into it. The situation continues till the upper bifurcation point $\beta = \frac{\rho(\sigma+K)^2}{4\sigma K}$, marking the region of bistability, is reached. Close to the Maxwell point, the travelling wave becomes very slow in a markedly nonlinear fashion. The transition from the pulled to the pushed wave occurs in the weak Allee effect regime, in agreement with the experimental observation of the transition in a laboratory population of budding yeast [11]. In the experiment, the 1d RD system was set up by culturing the yeast populations in linear arrays of wells on plates and through the exchange of small volumes of

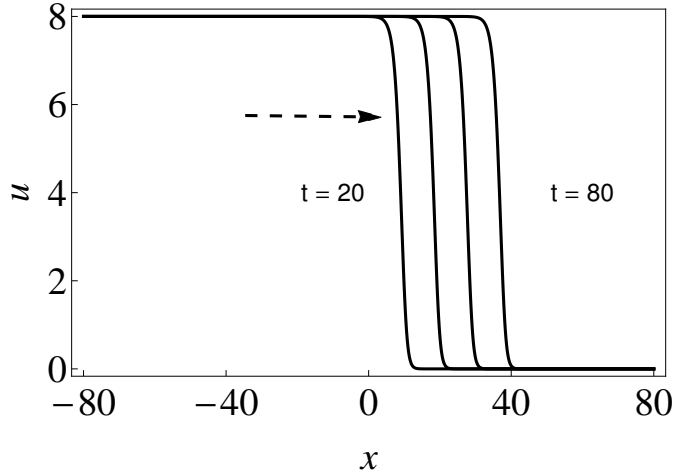


Fig. 3 Travelling wave solutions of the RD Eq. (1) with $F(u)$ given in Eq. (10) for $\alpha = 0$. The solutions are computed at the time points $t = 20, 40, 60$ and 80 . The other parameter values are $D = 1.0$, $\rho = 3.0$, $K = 12.0$, $\sigma = 2.0$, and $\beta = 5.0$.

the growth media between adjacent wells. In galactose or glucose growth medium, the Allee effect is absent so that the RD process is of the FKPP type with the travelling wave being a pulled wave with the front speed obeying the Luther scaling (Eq. (15)). In sucrose growth medium, the Allee dynamics come into play because the cooperative breakdown of sucrose into glucose is required for growth. The strength of the Allee effect was tuned by changing the relative concentrations of glucose and sucrose in the growth medium. The magnitude of the Allee effect was measured by the difference between the maximal and the low density growth rates. The transition from the pulled to the pushed wave was observed in the weak Allee regime as the Allee effect was made progressively strong. In our model study, the mortality rate constant β was changed to bring about the transition from the pulled to the pushed wave. Since this parameter is related to the dilution factor in the original yeast experiment of Dai *et al.* [8], our study suggests that the transition in the nature of the travelling front could also be tested by changing the dilution factor in the experimental RD system. The strong Allee regime would then correspond to the range of dilution factors in which the population density is bistable.

5. Conclusion

In this paper, we have studied a RD model in 1d with the Allee effect incorporated in the dynamics of the model. The model in its full form has not been studied previously. The strength of the model lies in the fact that the growth and the mortality rate constants appear explicitly as parameters in the model which are experimentally controllable. The model is general in nature and applicable for the study of population dynamics based on growth and diffusion. Though we could not derive analytical results for the full model, the results obtained through numerical computations are in agreement with the experimental observations on budding yeast populations. The model adds to the list of known models in population biology which investigate issues like population growth, extinction and range expansion. The knowledge of the early signatures of a tipping point transition to extinction (Sec. 3.1) would be of use in the eradication of harmful species like disease-causing bacteria, viruses and pathogens. Recent advances in cancer research have drawn parallels between tumour and population dynamics [12]. There is some experimental evidence that the Allee effect forms an important component in the dynamics of certain types of tumour. It is possible that many tiny tumours are formed in different parts of the body during the lifetime of an individual. Most of these tumours become extinct because of their small size, signifying a negative growth rate at low density as in the case of the Allee effect. It has been found that xenograft transplantations of cancer cells into mice with a functional immune system, are more likely to initiate tumours when the number of injected cells is large. The basis of the Allee effect may lie in cooperativity in the form of cancer cells contributing to a common pool of diffusible growth factors required for tumour proliferation. As emphasized in Ref. 12, the knowledge of the proximity of a tumour close to a growth threshold would facilitate in the alteration of drug doses. The detection of early signatures similar to the ones discussed in Sec. 3.1 could contribute in formulating therapeutic intervention protocols.

In the case of the full RD model with Allee-type dynamics, the existence of a travelling wave solution indicates the possibilities of both range expansion and retreat. The Allee effect makes it possible, by controlling the parameter values, to prevent the range expansion of harmful organisms or at least to slow down the speed of the spread. The containment of the pulled and pushed invasions requires different strategies: eradication of the invading population at the very edge of the expansion in the first case and eradication over the

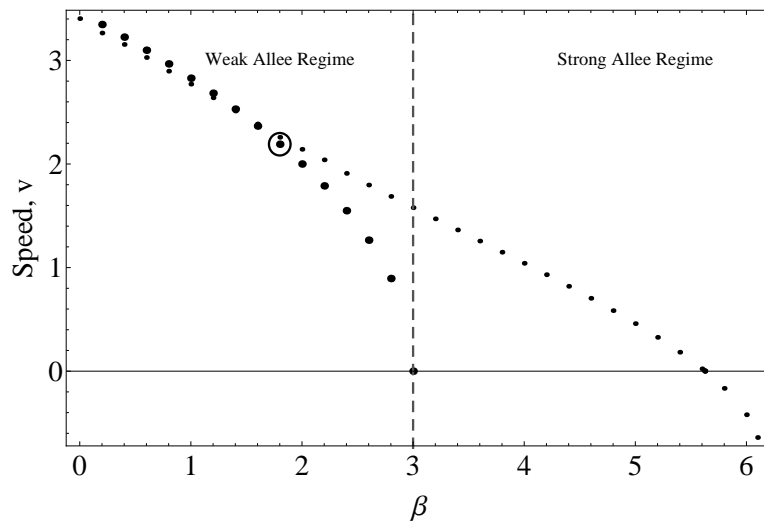


Fig. 4 Speed v versus β . The big open circle denotes the transition region from the pulled to the pushed wave. The larger solid black circles represent the speed of the pulled wave, $v = 2\sqrt{(\rho - \beta)D}$

entire invasion front in the second case. The RD model studied in the paper could be generalized to higher dimensions, say, $d = 2$ and a stochastic component included in the model. A recent study [24] indicates that in a 2d system, discontinuous transitions are of the type shown in Fig. 1 could be replaced by continuous transitions under the conditions of limited diffusion, enhanced noise and quenched spatial heterogeneity. Controlled experiments on laboratory populations of microbes may offer the opportunity to test some of the theoretical predictions.

Acknowledgments

IB acknowledges the support by CSIR, India, vide sanction Lett. No. 21 (0956)/13-EMR-II dated 28.04.2014. CK acknowledges the support by National Network for Mathematical and Computational Biology, India for carrying out part of the study. MP acknowledges support from Bose Institute, India for carrying out the research study.

References

1. M. C. Cross and P. C. Hohenberg, *Rev. Mod. Phys.* **65**, 851 (1993).
2. A. J. Koch and H. Meinhardt, *Rev. Mod. Phys.* **66**, 1481 (1994).
3. J. D. Murray, *Mathematical Biology I. An Introduction* (Springer-Verlag, New York, 2002).
4. M. A. Lewis, S. V. Petrovskii and J. R. Potts *The Mathematics Behind Biological Invasions* (Springer, Switzerland, 2016).
5. F. Courchamp, T. Clutton-Brock and B. Grenfell *Trends. Ecol. Evol.* **14**, 405 (1999).
6. A. Kramer, B. Dennis, A. Liebhold and J. Drake *Popul. Ecol.* **51**, 341 (2009).
7. L. Berec, E. Angelo and F. Courchamp *Trends Ecol. Evol.* **22**, 185 (2007).
8. L. Dai, D. Vorselen, K. S. Korolev and J. Gore *Science* **336**, 1175 (2012).
9. L. Dai, K. S. Korolev and J. Gore *Nature* **496**, 355 (2013).
10. M. Sen Datta, K. S. Korolev, I. Cvijovic, C. Dudley and J. Gore *Proc. Natl. Acad. Sci. (U.S.A)* **110**, 7354 (2013).
11. S. R. Gandhi, E. A. Yurtsev, K. S. Korolev and J. Gore *Proc. Natl. Acad. Sci. (U.S.A)* **113**, 6922 (2016).
12. K. S. Korolev, J. B. Xavier and J. Gore *Nat. Rev. Cancer* **14**, 371 (2014).
13. R. B. Kaul, A. M. Kramer, F. C. Dobbs and J. M. Drake *Biol. Lett.* **12**: 20160070 (2016).
14. M. A. Lewis and P. Kareiva *Theoret. Popul. Biol.* **43**, 141 (1993).
15. M. Scheffer *et al. Nature* **461**, 53 (2009).

16. M. Scheffer *et al.* *Science* **338**, 344 (2012).
17. M. Pal, A. K. Pal, S. Ghosh and I. Bose. *Phys. Biol.* **10**, 036010 (2013).
18. M. Pal, S. Ghosh and I. Bose. *Phys. Biol.* **12**, 016001 (2015).
19. R. A. Fisher *Ann. Eugen.* **7(4)**, 355 (1937).
20. S. V. Petrovskii and B-L. Li *Exactly solvable models of biological invasion* (Chapman and Hall, New York, 2006).
21. J. J. Tyson and J. P. Keener *PhysicaD* **32**, 327 (1988).
22. M. A. Tayar, E. Karzbrun, V. Noireaux and R. H. Bar-Ziv *Nature Physics* **11**, 1037 (2015).
23. P. C. Fife and J. B. McLeod *Arch. Rat. Mech. Anal.* **65**, 335 (1977).
24. P. Villa Martin, J. A. Bonachela, S. A. Levin and M. A. Muñoz *Proc. Natl. Acad. Sci. (U.S.A)* **112E**, 1828 (2015).